

Interaction of Fibrinogen with Fibronectin: Purification and Characterization of a Room
Temperature-Stable Fibrinogen-Fibronectin Complex from Normal Human Plasma

by

Ayman Ismail

A DISSERTATION

Presented to the Faculty of

The Graduate College at the University of Nebraska

In Partial Fulfillment of Requirements

For the Degree of Doctor of Philosophy

Major: Chemical and Biomolecular Engineering

Under the Supervision of Professor William H. Velandar

Lincoln, Nebraska

May, 2016

ProQuest Number: 10102326

All rights reserved

INFORMATION TO ALL USERS

The quality of this reproduction is dependent upon the quality of the copy submitted.

In the unlikely event that the author did not send a complete manuscript and there are missing pages, these will be noted. Also, if material had to be removed, a note will indicate the deletion.



ProQuest 10102326

Published by ProQuest LLC (2016). Copyright of the Dissertation is held by the Author.

All rights reserved.

This work is protected against unauthorized copying under Title 17, United States Code
Microform Edition © ProQuest LLC.

ProQuest LLC.
789 East Eisenhower Parkway
P.O. Box 1346
Ann Arbor, MI 48106 - 1346

Interaction of Fibrinogen with Fibronectin: Purification and Characterization of a Room Temperature-Stable Fibrinogen-Fibronectin Complex from Normal Human Plasma

Ayman E. Ismail, Ph.D.
University of Nebraska, 2016

Advisor: William H. Velandar

A fibrinogen-fibronectin complex ($\gamma\gamma'$ pdFI-pdFN) was purified from normal human plasma using a sequence of cryoprecipitation, ammonium sulfate fractionation, and DEAE Sepharose chromatography. Sodium dodecyl sulfate polyacrylamide gel electrophoresis (SDS-PAGE) under reducing condition showed both a 1:1 stoichiometric ratio of fibrinogen (FI) to fibronectin (FN) as well as a stoichiometric ratio of 1:1 of $\gamma\gamma$ to $\gamma\gamma'$. The $\gamma\gamma'$ pdFI-pdFN complex was non-covalent in nature as it was disrupted by affinity adsorption to Gelatin Sepharose where pdFN bound strongly and the disrupted $\gamma\gamma'$ pdFI fell through the chromatographic column. Surprisingly, the purified $\gamma\gamma'$ pdFI-pdFN complex was more broadly thermally stable than plasma FI (pdFI) preparations not containing plasma FN (pdFN) and was stable at physiologic pH, ionic strength and temperature.

The complex appeared as a compact species that was distinctly larger than pdFN alone when analyzed by high pressure size exclusion chromatography (HPSEC). Dynamic light scattering (DLS) showed that the native $\gamma\gamma'$ pdFI-pdFN complex is a more compact form at low ionic strength but adopt and extended conformation in high salt and denaturing conditions. DLS

also showed that FN decreased the degree of polydispersity and hydrodynamic radius of both $\gamma\gamma$ and $\gamma\gamma'$ FI, indicating that FN interact with both subspecies.

The clottability of the native $\gamma\gamma'$ pdFI-pdFN complex and mixtures of FN with unfractionated FI and FI subspecies was evaluated by Thromboelastography (TEG) assay. The $\gamma\gamma'$ pdFI-pdFN complex had appreciably enhanced clotting strength than comparable mixtures of FI and FN. FN had not effect on the polymerization rates of fibrin clots. FN, however, showed greater influence on the shear strength of fibrin clots even in the absence of factor FXIII mediated crosslinking. The maximal amplitude and shear strength increased over the entire range of FN concentrations for clots made from unfractionated FI and $\gamma\gamma'$ FI. FN had mixed effect on the rigidity of clots made from $\gamma\gamma$ FI. While high concentrations of FN enhanced the maximal amplitude and shear modulus, low concentrations decreased both factors.

The fibrin clots made from $\gamma\gamma'$ pdFI-pdFN showed a biological activity of human fibroblast and human umbilical vein endothelial cells (HUVEC) recruitment and adhesion *in vitro* exceeding that of fibrin made from equimolar concentration of pdFI and pdFN.

DEDICATION

This work is dedicated with gratitude to my amazing wife Isra and to my daughter Haneen.

PREVIEW

Acknowledgements

I would like to thank my advisor, Dr. William H. Velandar, for his guidance and encouragement throughout the project. Special thanks also to my committee members, Dr. Gustavo Larsen, Dr. Srivatsan Kidambi, Dr. Yuguo Lei, and Dr. Mark Carlson for their advice and support of this project.

I would like to gratefully acknowledge the generous encouragement of the late Dr. Bill Burgess, his technical advice and invaluable contribution to the success of this project. I would like to acknowledge Mostafa Fatemi, Jennifer Calcaterra, Weijie Xu, Nicholas Vanderslice, and Frank Fabian for their support, encouragement and guidance. I wish to thank Weijie Xu for reviewing and proofreading the document.

I am grateful to Dr. Mark Carlson for his gifts of human fibroblasts foreskin and human umbilical vein endothelial cells. I am indebted to Dr. Donald Becker for performing the analytical ultracentrifugation experiments and for his insightful discussions during the course of these experiments. Finally, I would like to thank Tiffany Peña for helping us with the cell adhesion studies.

Table of Contents

| | |
|---|-----|
| List of Tables | vi |
| List of Figures | vii |
| Chapter 1 INTRODUCTION..... | 1 |
| Fibrinogen | 2 |
| Purification of fibrinogen from human plasma | 6 |
| Fibronectin | 8 |
| Interaction of fibronectin with fibrinogen and fibrin | 13 |
| Dissertation objectives | 15 |
| References | 16 |
| Chapter 2 Purification and characterization of fibrinogen-fibronectin complex | 22 |
| Abstract | 23 |
| Introduction | 24 |
| Materials and Methods | 25 |
| Materials | 25 |
| Isolation of fibrinogen-fibronectin complex..... | 26 |
| SDS-PAGE Analysis | 28 |
| Western Blot Analysis | 29 |

| | |
|---|----|
| Dissociation of $\gamma\gamma'$ FI-FN complex by affinity Chromatography..... | 31 |
| Isolation of $\gamma\gamma$ and $\gamma\gamma'$ fibrinogen containing species..... | 31 |
| Results | 32 |
| Isolation and characterization of $\gamma\gamma'$ pdFI-pdFN complex | 32 |
| Gelatin Sepharose chromatography..... | 38 |
| Dissociation of $\gamma\gamma'$ pdFI-pdFN complex by affinity Chromatography..... | 39 |
| Isolation of $\gamma\gamma$ and $\gamma\gamma'$ fibrinogen containing species..... | 41 |
| Discussion | 43 |
| References | 46 |
| Chapter 3 Characterize the size distribution and hydrodynamic properties of the isolated $\gamma\gamma'$ pdFI-pdFN complex and comparable mixtures of FI and FN | 48 |
| Abstract | 49 |
| Introduction | 51 |
| Methods..... | 53 |
| Size Exclusion Chromatography | 53 |
| DLS..... | 53 |
| Analytical Ultracentrifugation..... | 54 |
| Statistical analysis..... | 55 |
| Results | 56 |

| | |
|---|----|
| SEC..... | 56 |
| Dynamic light scattering..... | 59 |
| Analytical Ultracentrifugation..... | 67 |
| Discussions..... | 74 |
| References | 77 |
| Chapter 4 Characterize the kinetics and viscoelastic properties of the isolated $\gamma\gamma'$ pdFI-pdFN complex and comparable mixtures of FI and FN..... | |
| Abstract | 80 |
| Introduction | 81 |
| Measuring the rheology of fibrin clots | 82 |
| Materials and Methods | 85 |
| Materials..... | 85 |
| Evaluating Clottability of FI-FN complex by Thromboelastography | 86 |
| Effect of FN on the clottability of FI..... | 86 |
| Statistical analysis..... | 87 |
| Results | 87 |
| Clottability of $\gamma\gamma'$ pdFI-pdFN complex by Thromboelastography | 87 |
| The effect of FN on the clotting of unfractionated pdFI | 89 |
| The effect of FN on the clotting of $\gamma\gamma$ and $\gamma\gamma'$ pdFI..... | 90 |

| | |
|---|-----|
| The effect of adding FN without crosslinking on the clotting of $\gamma\gamma$ and $\gamma\gamma'$ | 96 |
| The effect of FN on the clotting of $\gamma\gamma$ and $\gamma\gamma'$ rFI | 98 |
| Discussion | 101 |
| References | 104 |
| Chapter 5 Characterize the cell adhesion properties of the native $\gamma\gamma'$ pdFI-pdFN complex | 106 |
| Abstract | 107 |
| Introduction | 108 |
| Materials and Methods | 110 |
| Materials | 110 |
| Cell culture | 110 |
| Preparation of coated plate wells | 111 |
| Cell adhesion assays | 111 |
| Statistical analysis | 112 |
| Results | 112 |
| Discussion | 118 |
| References | 120 |
| Chapter 6 Examine the interaction of FN with FI by ligand blotting | 122 |
| Abstract | 123 |
| Materials and Methods | 124 |

| | |
|-------------------------------------|-----|
| Materials | 124 |
| Ligand blotting assay | 124 |
| Results | 125 |
| Interaction between FI and FN | 126 |
| Competition experiments | 126 |
| Discussion | 129 |
| References | 130 |

List of Tables

| | |
|--|-----|
| Table 1.1 Properties of fibrinogen | 3 |
| Table 1.2 list of some molecules that interact with fibrinogen and their physiological roles | 5 |
| Table 1.3 Properties of fibronectin | 9 |
| Table 1.4 molecules that interact with FN and their physiological functions | 11 |
| Table 3.1 DLS parameters of pdFN, pdFI, and $\gamma\gamma'$ pdFI-pdFN complex analyzed in 100 mM NaCl..... | 61 |
| Table 3.2 DLS parameters of pdFN, pdFI, and $\gamma\gamma'$ pdFI-pdFN complex analyzed in 1 M NaCl.. | 62 |
| Table 3.3 DLS parameters of pdFN, pdFI, and $\gamma\gamma'$ pdFN-pdFN complex analyzed in 6 M Urea. | 64 |
| Table 3.4 DLS parameters of pdFN, $\gamma\gamma$ pdFI, $\gamma\gamma'$ pdFI, $\gamma\gamma'$ pdFI-pdFN complex, and mixtures of pdFN with $\gamma\gamma$ pdFI and $\gamma\gamma'$ pdFI species analyzed in 150 mM NaCl. | 66 |
| Table 4.1 Kinetics and viscoelastic parameters of clots from pdFI and $\gamma\gamma'$ pdFI-pdFN complex. | 88 |
| Table 4.2 Kinetics and Viscoelastic parameters of clots from unfractionated pdFI..... | 90 |
| Table 4.3 Kinetics and viscoelastic parameters of clots from mixtures of $\gamma\gamma'$ pdFI and FN | 92 |
| Table 4.4 Kinetics and viscoelastic parameters of clots from mixtures of $\gamma\gamma$ pdFI and FN | 93 |
| Table 4.5 Viscoelastic and kinetic parameters of clots from the native and reconstituted $\gamma\gamma'$ pdFI-pdFN complex. | 95 |
| Table 4.6 Kinetics and viscoelastic parameters of clots from $\gamma\gamma$ and $\gamma\gamma'$ pdFI with or without FXIII and pdFN | 97 |
| Table 4.7 Kinetics and viscoelastic parameters of clots from mixtures of $\gamma\gamma'$ rFI and FN..... | 99 |
| Table 4.8 Kinetics and viscoelastic parameters of clots from mixtures of $\gamma\gamma$ rFI and FN | 100 |

List of Figures

| | |
|---|----|
| Figure 1.1 Schematic diagram of the structure of human fibrinogen. The domains and subunits are shown. The figure is adopted from reference [1] | 3 |
| Figure 1.2 Schematic representation of the structure of human fibronectin..... | 10 |
| Figure 1.3 Schematic representation of the interaction of the N-terminal Fib-1 region with the α C domain. | 15 |
| Figure 2.1 Purification procedure of fibrinogen-fibronectin complex..... | 30 |
| Figure 2.2 Gel electrophoresis evaluation of plasma fibrinogen purified by cryoprecipitation and ammonium sulfate precipitation. | 33 |
| Figure 2.3 Fractionation of ammonium sulfate precipitated pdFI on DEAE Sepharose chromatography. | 34 |
| Figure 2.4 Gel electrophoresis evaluation of plasma fibrinogen-fibronectin complex purified by DEAE Sepharose chromatography. | 35 |
| Figure 2.5 Native gel electrophoresis analysis of $\gamma\gamma'$ pdFI-pdFN complex..... | 36 |
| Figure 2.6 Anti-fibrinogen (A) and anti-fibronectin (B) western blot analyses of $\gamma\gamma'$ pdFI-pdFN complex. | 37 |
| Figure 2.7 Anti-fibrinogen alpha chain (A), anti-fibrinogen beta chain (B), and anti-fibrinogen gamma chain (c) Western Blot analyses of $\gamma\gamma'$ pdFI-pdFN complex..... | 37 |
| Figure 2.8 Fractionation of ammonium sulfate precipitated fibrinogen on gelatin Sepharose chromatography. | 39 |
| Figure 2.9 Disruption of $\gamma\gamma'$ pdFI-pdFN complex by affinity chromatography on gelatin Sepharose..... | 40 |

| | |
|---|----|
| Figure 2.10 Gel electrophoresis evaluation of disrupting plasma $\gamma\gamma'$ pdFI-pdFN complex on gelatin Sepharose chromatography..... | 41 |
| Figure 2.11 Isolation of $\gamma\gamma$ and $\gamma\gamma'$ fibrinogen subspecies by DEAE Sepharose chromatography. | 42 |
| Figure 2.12 Gel electrophoresis analysis of $\gamma\gamma$ and $\gamma\gamma'$ fibrinogen subpopulation resolved by DEAE Sepharose. | 43 |
| Figure 3.1 Block diagram of DLS instrument | 52 |
| Figure 3.2 size exclusion chromatography of pdFN, isolated complex, $\gamma\gamma$ and $\gamma\gamma'$ pdFI species. | 57 |
| Figure 3.3 Size exclusion chromatography of a mixture of $\gamma\gamma'$ pdFI and pdFN..... | 58 |
| Figure 3.4 Size exclusion chromatography of a mixture of $\gamma\gamma$ pdFI and pdFN. | 59 |
| Figure 3.5 Size distribution of pdFN and $\gamma\gamma'$ pdFI-pdFN complex. | 61 |
| Figure 3.6 Size distribution of pdFN, pdFI, and $\gamma\gamma'$ pdFI-pdFN complex..... | 62 |
| Figure 3.7 Size distributions of pdFN, pdFI, and $\gamma\gamma'$ pdFI-pdFN complex. | 64 |
| Figure 3.8 Size distributions of pdFN, $\gamma\gamma$ pdFI, $\gamma\gamma'$ pdFI, $\gamma\gamma'$ pdFI-pdFN complex, and mixtures of pdFN with $\gamma\gamma$ pdFI and $\gamma\gamma'$ pdFI. | 66 |
| Figure 3.9 Sedimentation velocity data of pdFN. | 69 |
| Figure 3.10 Sedimentation velocity data of $\gamma\gamma'$ pdFI. | 69 |
| Figure 3.11 Sedimentation velocity data of the isolated $\gamma\gamma'$ FI-FN complex. | 70 |
| Figure 3.12 Sedimentation velocity data of an equimolar mixture of $\gamma\gamma'$ pdFI and pdFN. | 70 |
| Figure 3.13 Sedimentation velocity data of an equimolar mixture of $\gamma\gamma$ pdFI and pdFN..... | 71 |
| Figure 3.14 Sedimentation equilibrium data of unfractionated pdFI..... | 72 |
| Figure 3.15 Sedimentation equilibrium data of pdFN. | 73 |
| Figure 3.16 Sedimentation equilibrium data of $\gamma\gamma'$ pdFI-pdFN..... | 73 |

| | |
|---|-----|
| Figure 3.17 Sedimentation equilibrium data of a mixture of $\gamma\gamma'$ pdFI and pdFN..... | 74 |
| Figure 3.18 schematic diagram of $\gamma\gamma$ and $\gamma\gamma'$ interactions with FN. | 76 |
| Figure 4.1 TEG tracing parameters..... | 85 |
| Figure 4.2 Thromboelastography analysis of clots formed from pdFI and native $\gamma\gamma'$ pdFI-pdFN complex. | 88 |
| Figure 4.3 Thromboelastography analysis of clots formed from unfractionated pdFI. | 90 |
| Figure 4.4 Thromboelastography analysis of clots formed from mixtures of $\gamma\gamma'$ pdFI and pdFN. | 92 |
| Figure 4.5 Thromboelastography analysis of clots formed from mixtures of $\gamma\gamma$ pdFI and pdFN.. | 93 |
| Figure 4.6 Thromboelastography comparison of clots formed from the native and reconstituted $\gamma\gamma'$ pdFI-pdFN complex..... | 95 |
| Figure 4.7 Thromboelastography analysis of clots formed from $\gamma\gamma$ and $\gamma\gamma'$ pdFI with or without FXIII and pdFN. | 97 |
| Figure 4.8 Thromboelastography analysis of clots formed from mixtures of $\gamma\gamma'$ rFI and pdFN.... | 99 |
| Figure 4.9 Thromboelastography analysis of clots formed from mixtures of $\gamma\gamma$ rFI and pdFN. . | 100 |
| Figure 4.10 Effect of FN on the shear modulus of clots made from unfractionated FI and fractionated $\gamma\gamma$ and $\gamma\gamma'$ FI as determined by TEG..... | 101 |
| Figure 5.1 Fibroblasts adhesion to A) propylene; B) fibrin clots formed from plasma pdFI; C) fibrin clots formed from equimolar concentration of pdFI and pdFN; D) fibrin clots formed from the isolated $\gamma\gamma'$ pdFI-pdFN complex..... | 114 |
| Figure 5.2 HUVECs adhesion to: A) propylene; B) fibrin clots formed from pdFI; C) fibrin clots formed from equimolar concentration of pdFI and pdFN; D) fibrin clots formed from $\gamma\gamma'$ pdFI-pdFN complex..... | 115 |
| Figure 5.3 Quantitation of fibroblasts cells attachment. | 116 |

| | |
|--|-----|
| Figure 5.4 Quantitation of HUVEC cells attachment. | 116 |
| Figure 5.5 Time course of fibroblasts cells adhesion. | 117 |
| Figure 5.6 Time course of HUVECs cells adhesion. | 117 |
| Figure 6.1 Anti-fibronectin (A) and anti-fibrinogen γ' -chain (B) Western blot analysis of fibrinogen..... | 127 |
| Figure 6.2 Gel electrophoresis (A) and ligand blotting analysis (B) of fibrinogen. | 128 |
| Figure 6.3 Ligand blot analysis of fibronectin binding to immobilized fibrinogen and fibrinogen in solution. | 128 |

Chapter 1 INTRODUCTION

PREVIEW

Fibrinogen

Fibrinogen (FI), the main component of the hemostatic system, is transformed by thrombin into fibrin monomers which spontaneously polymerizes forming a clot that fills the wound and prevent the loss of blood. In addition to preserving the integrity of the vascular system, the clot also initiates the wound healing process by functioning as a provisional matrix for cell adhesion and migration into the injured tissue [4]. Furthermore, because it has multiple binding sites that can react with other proteins, FI plays important roles in many physiological and pathological processes including fibrinolysis, cell adhesion, inflammation, angiogenesis, atherogenesis, tumorigenesis, and wound healing.

Fibrinogen is a 340 kDa glycoprotein containing two identical subunits, each is made of three different polypeptide chains termed $A\alpha$, $B\beta$, and γ [5, 6] (Figure 1.1). A series of disulfide bonds link fibrinogen polypeptide chains forming elongated 45 nm tri-nodular structures with several distinct domains. These domains are arranged into three main structural regions: a central E, two distal D and the αC regions. The central E nodule is formed by the N-terminal portions of the six polypeptide chains. The distal D nodules, formed by the C-terminal portions of the $B\beta$ and γ as well as a fraction of the $A\alpha$ chains, are separated from the E region by coiled-coil regions [7, 8]. The C-termini of the two $A\alpha$ -chain, known as the αC domains, have been shown to extends freely into solution or associate noncovalently with the central nodule [9]. The properties of the fibrinogen molecule are listed in Table 1.1.

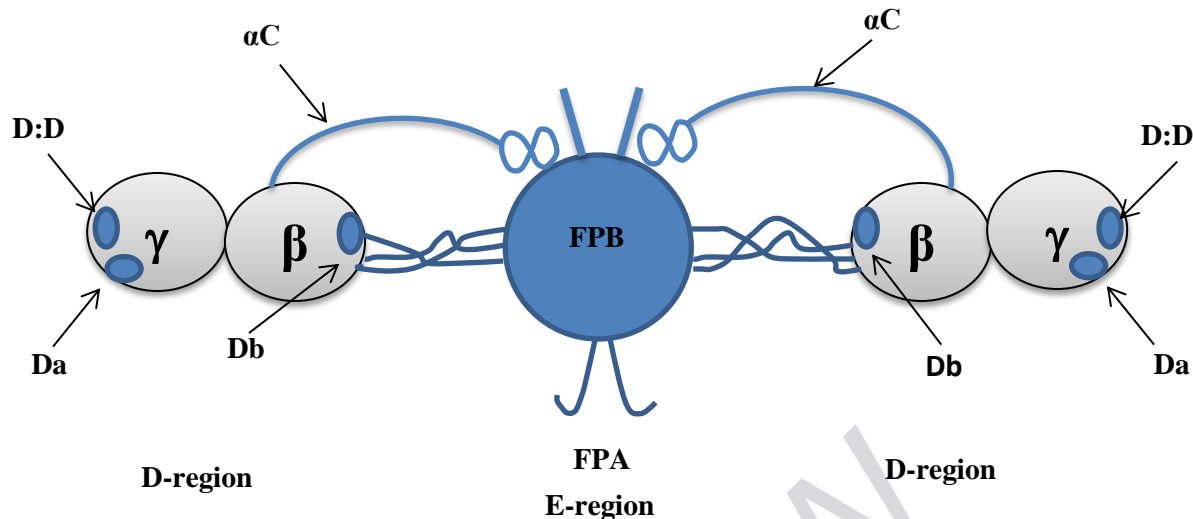


Figure 1.1 Schematic diagram of the structure of human fibrinogen. The domains and subunits are shown. The figure is adopted from reference [1]

Table 1.1 Properties of fibrinogen

| | |
|-----------------------------------|--|
| Molecular weight [10] | 340 kDa |
| Subunits | Two A α , two B β , and two γ |
| Amino acids [11] | 610 A α , 461 B β , 411 γ |
| Synthesized by | Primarily hepatocytes and secondarily platelets |
| Plasma concentration | 2-4 mg/ml |
| Carbohydrate [12] | 3% of total weight, consist of Sia, Gal, Man, and GlcNAc sugars |
| Isoelectric point [13] | 5.8 |
| Diffusion coefficient [14] | $2 \times 10^{-7} \text{ cm}^2 \text{ s}^{-1}$ in ionic strength of 0.15 M and pH 7.35 |

The A α , B β , and γ polypeptide chains of human fibrinogen are encoded by three separate genes [15]. The three genes are closely linked as a cluster in a region of 50-kilobase on

chromosome 4q31.3. The A α gene is in the middle and surrounded by the B β gene from one side and the γ -gene on the other. The A α and B β genes are produced by simple transcription events, whereas plasma γ gene is generated by complex transcriptional event that involve differential RNA splicing and polyadenylation [16, 17].

Human FI heterogeneity results from variant splicing, phosphorylation or glycosylation, and a number of genetic polymorphisms [18]. The heterogeneity occurs naturally when FI is partially degraded during circulation to low molecular weight species with 305 kDa and 270 kDa with one or two of A α -chains partially degraded at the c-terminus, respectively [19-21]. The heterogeneity is also due in part to the presence of a minor variant form of the γ -chain, known as γ' . The γ' -chain accounts for about 5-15% [22, 23] of normal human plasma fibrinogen and is formed by the alternative processing of the primary mRNA transcript [24, 25]. Amino acid sequence analysis has demonstrated the replacement of 4 amino acids (AGDV) in the C-terminal of the γ -chain with a unique 20 amino acid sequence [26] that contains two sulfated tyrosines and several Asp and Glu residues. Therefore, the γ' -chain is longer, contains more anion groups, and has higher molecular weight than the γ -chain. It has been reported that the γ' -chain bind to the B subunit of factor XIII (FXIII) and serves as a carrier for FXIII in plasma [27].

Fibrinogen has the ability to interact with numerous substances with important physiological consequences. For example, The C-terminal of the A α -chain (α C domains) of fibrinogen has binding sites for α_2 -AP, plasminogen, tissue-type plasminogen activator (tPA), and PAI-2. Table 1.2 lists binding sites and physiological roles of some fibrinogen-protein interactions.

Table 1.2 list of some molecules that interact with fibrinogen and their physiological roles

| Ligands | Binding site | Function |
|--------------------------------------|--------------------------------|------------------------------------|
| Fibronectin [28] | A α -chain | Cell adhesion |
| Lipoprotein (a) [29] | - | Proliferation of endothelial cells |
| Thrombin [30] | γ' -chain | Inhibit fibrinolysis |
| Plasminogen [31, 32] | A α -chain | Enhance fibrinolysis |
| FXIII [27] | γ' -chain | Clot stabilization |
| α_2-AP [33] | A α -chain | Fibrinolysis resistance |
| Integrin [34] | A α -chain | Cellular interactions |
| Calcium | B β and γ -chains | Promote polymerization |
| Heparin [35-37] | B β -chain | Cell-matrix interactions |

During coagulation, thrombin converts soluble fibrinogen into fibrin monomers, which then polymerize to form a network of fibrin fibers. This network is stabilized by thrombin activated FXIII to form an insoluble fibrin clot. Formation of fibrin begins when thrombin binds to a substrate site in fibrinogen and cleaves fibrinopeptides A (FpA) and B (FpB) from the amino termini of the A α and B β chains, respectively. The removal of FpA exposes the polymerization site “A” that contains the N-terminal sequence Gly-Pro-Arg-Val of the A α -chain, while the removal of FpB exposes the polymerization site “B” that contains the N-terminal sequence Gly-His-Arg-Pro of the B β -chain [38]. The polymerization site “A” interacts with the complementary binding site of the γ -chain, whereas the polymerization site “B” interacts with the complementary binding site of the β chain. These interactions lead to the formation of half-staggered, double-stranded protofibrils that undergo lateral aggregation to form fibrils [39-42].

The resulting fibrils also undergo lateral aggregation forming three-dimensional fiber matrix [43, 44]. Thrombin simultaneously converts FXIII to the active form (FXIIIa) which catalyzes the formation of covalent ϵ -(γ -glutamyl) lysine bonds between adjacent fibrin molecules. The cross-linking occurs rapidly between Lys-406 of one γ -chain and Gln-398 of another γ -chain to form γ -dimers [45-47]. FXIIIa also catalyzes the formation of slowly developing ϵ -(γ -glutamyl) lysine linkages between amine donor and lysine acceptor in the α -chains [48, 49] resulting in oligomers and larger polymers [50-52]. In addition, ϵ -(γ -glutamyl) lysine bonds also occur between α and γ chains [43, 53] as well as γ and γ chains leading to formation of hetero-dimers cross-linked α - γ [54], γ trimmers, and γ tetramers [43, 51, 53, 55].

Purification of fibrinogen from human plasma

Different techniques have been developed for the purification of fibrinogen from plasma materials. Cryoprecipitation is the most common method for isolating fibrinogen, which reduces the solubility of fibrinogen at lower temperature to prevent its denaturation. Compared to fresh frozen plasma, cryoprecipitate contains an increased percentage of fibrinogen. Cryoprecipitation involves freezing the citrated plasma at lower temperature, usually $-20\text{ }^{\circ}\text{C}$ or less for at least 12 hours. The frozen plasma is slowly thawed at $4\text{ }^{\circ}\text{C}$ followed by centrifugation to isolate the fibrinogen precipitate. The concentration of fibrinogen produced by cryoprecipitation is between 8 to 30 mg/ml and can be increased to 40 to 60 mg/ml using repeated freeze/thaw cycles. An ultrafiltration procedure has been used to purify fibrinogen where platelet rich plasma is separated using an ultrafiltration chamber with a molecular weight cutoff of 30 kDa. Fibrinogen obtained using this method has a final concentration of 6 mg/ml and lower clottability due to large amount of fibrinogen being denatured. Fibrinogen has also been isolated from human

plasma by using chemical precipitation methods in which chemical agents such as ethanol, glycine, β -alanine, ether, or ammonium sulfate are used to precipitate fibrinogen from plasma.

The clinical use of fibrinogen from pooled human plasma has been previously associated with a high risk of transmission of plasma-borne infectious species such as HIV, HBV, and HCV. The improvements in viral testing and screening have reduced, but not eliminated this risk. Therefore, different techniques have been developed in order to inactivate pathogenic viruses in fibrinogen derived from human plasma. Dry heat treatment at 60-68 °C of plasma cryoprecipitate inactivates HIV but it does not prevent the transmission of HCV. Plasma pathogens have been inactivated by treating fresh plasma with methylene blue followed by exposure to visible light. This approach is less effective versus non-enveloped viruses and results in approximately 20% fibrinogen loss. Solvent detergent treatment is the most effective procedure for inactivating blood-borne lipid-enveloped viruses. Solvent detergent treatment inactivates viruses by dissolving their lipid envelope but it does not inactivate non-lipid enveloped viruses such as parvovirus or hepatitis A virus. The treatment of cryoprecipitate with a combination of organic solvent, tri (n-butyl) phosphate (TNBP), and detergent (sodium cholate, Tween 80, or Triton X-100) has been shown to inactivate very large quantities of HBV, HCV, and HIV while preserving the activity of the purified protein. Radosevich et al showed that treating cryoprecipitate with a mixture of 0.3% TNBP and 1% tween 80 at 25 °C for 6 hours inactivated $\geq 5.5 \log_{10}$ of HIV, $\geq 5 \log_{10}$ of VSV virus, and $\geq 6.5 \log_{10}$ of sindbis virus [56]. Horowitz and coworkers revealed that subjecting pooled plasma to a mixture of 1% TNBP and 1% Triton X-100 for 4 hours at 30 °C inactivates $\geq 10^6$ CID₅₀ of HBV, 10^5 CID₅₀ of HCV, and $10^{6.2}$ TCID₅₀ of HIV.

Fibronectin

Fibronectin (FN) is a large, multifunctional, adhesive glycoprotein that is present in a soluble form in plasma or as insoluble filaments deposited on the extracellular matrix (ECM) [57]. It regulates cellular processes and deposited by cells into a provisional ECM where it functions as a scaffold to maintain and direct tissue organization [58]. FN incorporated into fibrin by FXIII mediates interaction of fibrin with cells or platelets during clot formation. Bound fibronectin forms a three-dimensional matrix at the wound site that attracts different cell types and ECM proteins.

FN is secreted as a dimer composed of two nearly identical polypeptides chains each with a molecular weight of ~220-250 kDa [59-61] that are linked together by two disulfide bonds located close to the C-terminal region [62, 63]. Each polypeptide chain is made of three types of repeating modular consensus amino acid sequences known as types I, II, and III (F1, F2, and F3) [64]. FN properties are listed in Table 1.3. There are 12 type I modules, two type II modules, and 15-17 type III modules, which together accounts for ~90% of the fibronectin sequence. Type I modules contain ~45 amino acids held together by two disulfide bonds and located in the amino and carboxyl termini regions of each subunit. Type II modules are composed of ~60 amino acids linked by two disulfide bonds and localized in the gelatin binding domain of the subunit. Type III modules consists of ~90 amino acids that are clustered together in the middle of the subunit and does not contain disulfide bonds. The N-terminal region of fibronectin consist of five type I modules whereas the C-terminal contains three type I modules. These modules are organized into well-defined functional domains that include the 70 kDa N-terminal domain, the 120 kDa central binding domain, and the heparin binding domain. Fibronectin domains are shown in Figure 1.2.